(Proceedings ModelCARE2011 held at Leipzig, Germany, in September 2011) (IAHS Publ. 355, 2012).

Reducing hydrograph uncertainty through subsurface characterization

STEVEN B. MEYERHOFF & REED M. MAXWELL

Colorado School of Mines, Hydrologic Science and Engineering Program, Integrated GroundWater Modelling Centre, 1516 Illinois Street, Golden, Colorado, USA

smeyerho@mines.edu

Abstract Subsurface heterogeneity in saturated hydraulic conductivity is one of the largest sources of uncertainty in hydrology and hydrogeology. However, recent work has demonstrated that uncertainty in hydraulic conductivity can also impart significant uncertainty in runoff processes. Here, the role of site characterization in reducing hydrograph uncertainty and bias is demonstrated numerically. A fully integrated hydrologic model is used in a hypothetical experiment where a control hillslope is generated using correlated, Gaussian random fields. Direct measurements of hydraulic conductivity at varying density are obtained from this control simulation and assimilated into stochastic transient simulations. The hydrographs, resulting from integrated flow simulations for each realization, are shown to much more accurately match the control. Data assimilation resolves large-scale features in surface ponding and saturation. This implies that substantial reduction in hydrograph uncertainty may be reached through site characterization.

Key words conditioning; groundwater surface water interactions; hillslope; runoff generation

INTRODUCTION

We use a fully-integrated hydrologic model, ParFlow (Ashby & Falgout, 1996; Jones & Woodward, 2001; Kollet & Maxwell, 2006), that simultaneously solves for variably saturated subsurface flow and surface overland flow using fine-scale, structured, geostatistical heterogeneity to determine how saturated hydraulic conductivity assimilation affects runoff predictions. We adopt a Monte Carlo approach where a large number of subsurface realizations based upon assimilated data, represent our uncertainty about the spatial location of hydraulic conductivity values, and are used to generate parameter values for this integrated flow model and distributions of outflow. We present how assimilated saturated hydraulic conductivity data reduces subsurface uncertainty and how this reduction propagates to runoff prediction.

This work presented here seeks to answer the following research questions:

(1) Does a reduction in the subsurface hydraulic conductivity uncertainty propagate to runoff?
(2) Does subsurface hydraulic conductivity conditioning differ for Hortonian *versus* Dunne flow dominated systems?
(3) Does reducing subsurface permeability uncertainty propagate to other runoff mechanisms such as saturation and pressure head?
(4) Do we see the same structural errors both temporally and spatially for baseflow and overland flow?

An idealized hillslope with uniform, unit rainfall was specified to specifically isolate the role of the spatial distribution of and uncertainty in hydraulic conductivity on outflow. Outflow results were averaged over the ensemble and descriptive statistics were calculated. Two different water table initializations were used to isolate differences in the role of heterogeneity on runoff production for subsurface dominated flow (Dunne flow) and overland flow (Hortonian flow) cases. This work (1) addresses the uncertainty in hydraulic conductivity by assimilating known data into ensembles of model simulations; and (2) uses the assimilated data to address how known information reduces the uncertainty in runoff. The basic approach is as follows: a fully-3D hillslope with Gaussian, correlated-random heterogeneity fields is used to simulate runoff under Hortonian (overland-only) and Dunne (mixed overland-subsurface); a single case is used as a control scenario where known data is assimilated into ensembles of realizations for each case (overland flow, and mixed overland-subsurface flow), and these ensemble simulations are used to address the uncertainty in hydraulic conductivity and its role on runoff mechanisms.

METHODS

Data analysis

In this study we look at outflow, land surface saturation and pressure head. To represent the differences and uncertainty between the control scenario and the conditional cases we use the residual, and root mean squared residual.

Non-dimensionalization

A series of non-dimensional variables are used to generalize the simulation results and to make it easier for comparison studies. The variables used here are the same as those developed in Maxwell & Kollet (2008). The primary variable that is non-dimensionalized is qr' which is the rain rate (*Qrain*) normalized by the geometric mean of permeability in the domain, K_g. This variable is a basis for analysis for the baseflow and overland cases. A non-dimensional time, t', is also used, which is defined as the total time normalized by the time of rain application. The model dimensions were also non-dimensionalized, as well as Manning's coefficient. These can be seen below:

$$qr' = \frac{Qrain}{K_g}, \mathrm{t}' = \frac{t}{t_a}, x' = \frac{x}{k_g t_a}, y' = \frac{y}{k_g t_a}, z' = \frac{z}{k_g t_a}, n' = n\left(\frac{t_a}{(k_g t_a)^{1/3}}\right)$$

Control scenario

ParFlow was used to create an idealized, detailed hillslope-scale domain. The model represents hillslope domain of $x' = y' = 3000$ and $z' = 30$. The domain was wedge-shaped to allow for the initialization of the water table at a specified depth. The grid dimensions used were $dx' = dy' = 50$ and $dz' = 0.2$ resulting in nx = ny = 60 and nz = 300, for a total size of 1.08 million compute cells. The saturated hydraulic conductivity was populated using Gaussian correlated random fields as has been used frequently in past hydrogeological studies (Tompson *et al.*, 1989; Rubin, 2003; Rubin & Dagan, 1992), specifically using the Turning Bands Algorithm (Tompson *et al.*, 1989). Constant van Genuchten (van Genuchten, 1980) parameters were used to describe the pressure–saturation relationship used to solve Richards' equation. Bedslopes were set to $S_{f,x} = -0.005$ and $S_{f,y} = 0.0$ with and a constant non-dimensional Manning's n' of 2.32×10^{-6}. The specified slopes allow for overland flow in the x direction only.

Rain was applied over the entire domain for a $\Delta t' = 1$ and a recession period of $\Delta t' = 1$ for all cases, with an additional recession period of $\Delta t' = 5$ for baseflow cases. For the overland cases, the water table is initialized at the base of the domain to allow for Hortonian runoff flow only.

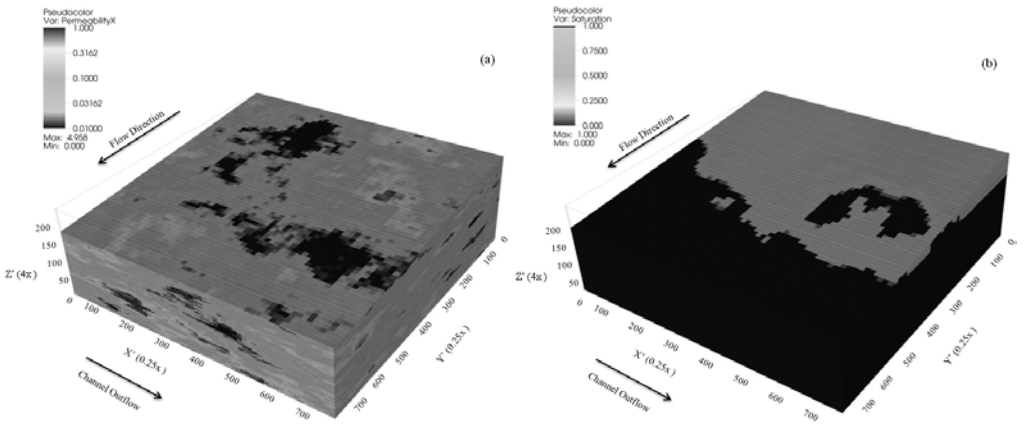

Fig. 1 Problem schematic and representation of (a) one heterogeneity realization and (b) resulting saturation pattern. Note the log scale in permeability, where black is low permeability and grey is high permeability. Also, note the X and Y-axis have an exaggeration of 0.25× and Z axis of 4×.

However, for baseflow cases the water table was initialized at the slope base to allow for a mixture of Dunne and Hortonian flow. The water table locations are the only initial conditions applied over the domain. Boundary conditions in the domain are no flow on all *x–y* subsurface faces except for the land surface, where there is an overland flow boundary condition. Overland flow is allowed to leave the domain, while subsurface flow in the *Xmax* face is considered to be at the channel a point of symmetry in our configurations. Figure 1 shows a representation of hillslope permeability (a) and subsequent coupled flow simulation, a snapshot in time of the saturation during rainfall (b). This figure is also a problem schematic that shows the flow direction and outlet location.

Conditional simulations

Hydraulic conductivity was directly sampled from the top one metre of soil at regular intervals from the control case and these points are used as the basis for a suite of conditional ensembles. The same global geostatistics were used in the conditional simulations (i.e. the mean, variance and correlations lengths were assumed to be known) as the control scenario but with increasing amounts of assimilated data. This resulted in eight cases, unconditional (zero conditioning points), 75, 150 and 300 conditioning points for the baseflow and overland flow initial conditions. For each case, baseflow and overland (unconditional, 75, 150 and 300), 50 equally-likely realizations of hydraulic conductivity were simulated and a full transient flow simulation was conducted. These equally-likely realizations all contain the same global statistics – mean, variance and correlation structure – but have a different spatial arrangement of hydraulic conductivity values dependent on a random seed and assimilated data. Simulation results, such as the outflow hydrograph, saturation and pressure head, were averaged over all 50 realizations.

RESULTS AND DISCUSSION

Here, we only show the results for the CTRL, unconditional and 300 points cases for brevity. Figure 2 shows the hydraulic conductivity fields for the CTRL, unconditional and 300 points cases for the land surface. All cases are averaged across all 50 realizations, creating an ensemble average saturated hydraulic conductivity for each land surface cell. The unconditional case average shows the geometric mean of saturated hydraulic conductivity across the entire land surface. At the 300 points data level the large-scale features of land surface hydraulic conductivity are more closely represented. For the unconditional case the residual errors are large in areas where there are

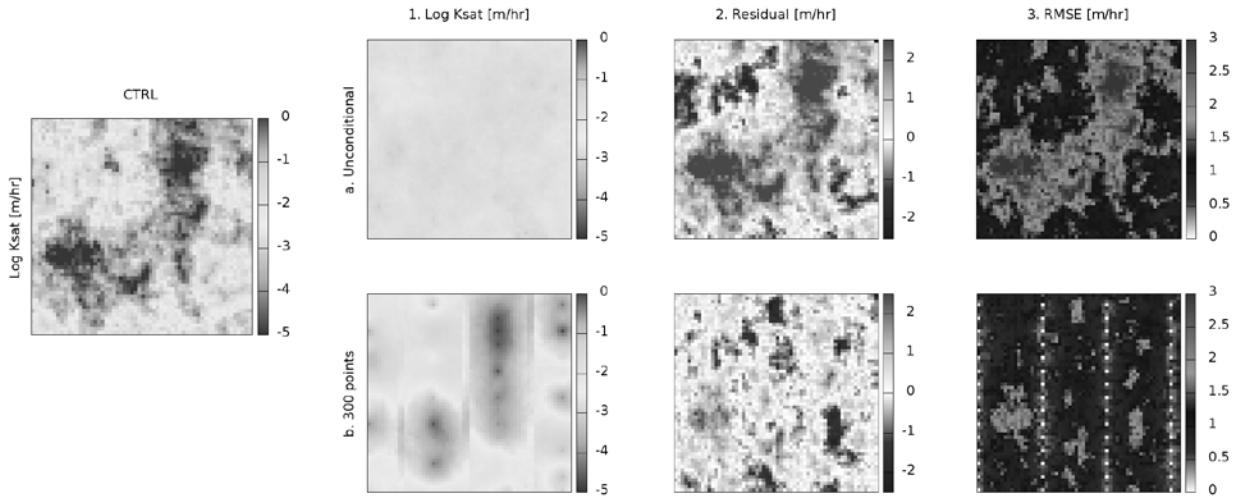

Fig. 2 Saturated hydraulic conductivity for the land surface for the CTRL (side image) and averaged for ensemble results in column 1 a and b. Column 2 shows the residual between the averaged conditional saturated hydraulic conductivity and the CTRL case and column 3 shows the RMSE. Saturated hydraulic conductivities are shown in log space. Note the mean squared residuals are plotted on a log scale.

variations from the geometric mean of saturated hydraulic conductivity. The 300 conditional cases show a reduction in residual errors at the land surface locations of sampling and the surrounding areas within the correlation lengths. In each conditional case (Fig. 2(1a,1b) there is distinct banding in the land surface saturated hydraulic conductivity. This is a function of the maximum search radius in the kriging algorithm. The conditioning scheme that was chosen represents the general patterns of the low and high conductivity zones in the 300 points very well but does not represent the small-scale heterogeneities; which is a function of averaging over 50 realizations. Conditioning saturated hydraulic conductivity allows for the interrogation of runoff, land surface saturation and pressure head to determine how reduction in error and uncertainty of hydraulic conductivity propagates to these variables. Below, we connect how reducing uncertainty in saturated hydraulic conductivity in baseflow and overland cases affects the spatial and temporal signals of runoff, land surface pressure and saturation.

At every time step we interrogated land surface pressure head and saturation. For each variable the residual and root mean squared residual are interpreted to determine how subsurface characterization of saturated hydraulic conductivity propagates to these variables. We will focus on the ensemble-averaged predictions of land-surface variables. Different spatial structures of error are seen at different times and for different cases (baseflow or overland). In baseflow cases, ponding happens very quickly and covers a significant portion of the hillslope; Fig. 3 shows the land surface pressure head at a t/ta = 1.0 for the baseflow case. Reducing subsurface uncertainty upslope (near the hillslope maximum) propagates downslope; which is prevalent in the 300 points case residuals (Fig. 3). With increasing data assimilation the large scale heterogeneities of pressure head are resolved more finely. In the overland cases, the same propagation of error downslope is not seen (Fig. 4). Error reduction is seen in areas where the low saturated hydraulic conductivity zones are more resolved. Hortonian flow is more likely to occur on low saturated hydraulic conductivity than on high-saturated hydraulic conductivity areas. Determining these low conductivity zones is crucial for prediction in overland flow cases. In both Fig. 3 and Fig. 4 data assimilation results in a better prediction of the large-scale heterogeneities. We also see an under prediction of ponding in the maximum ponding areas and an over prediction in small ponding areas.

In land surface saturation for baseflow cases, Fig. 5 (t/ta = 4.0), the residual errors have the same spatial structure as the saturated hydraulic conductivity, where the water table has not interacted with the land surface. In each conditioning case the ensemble average land surface saturation dries out quicker than the CTRL case. For overland land surface saturation (t/ta = 2.0,

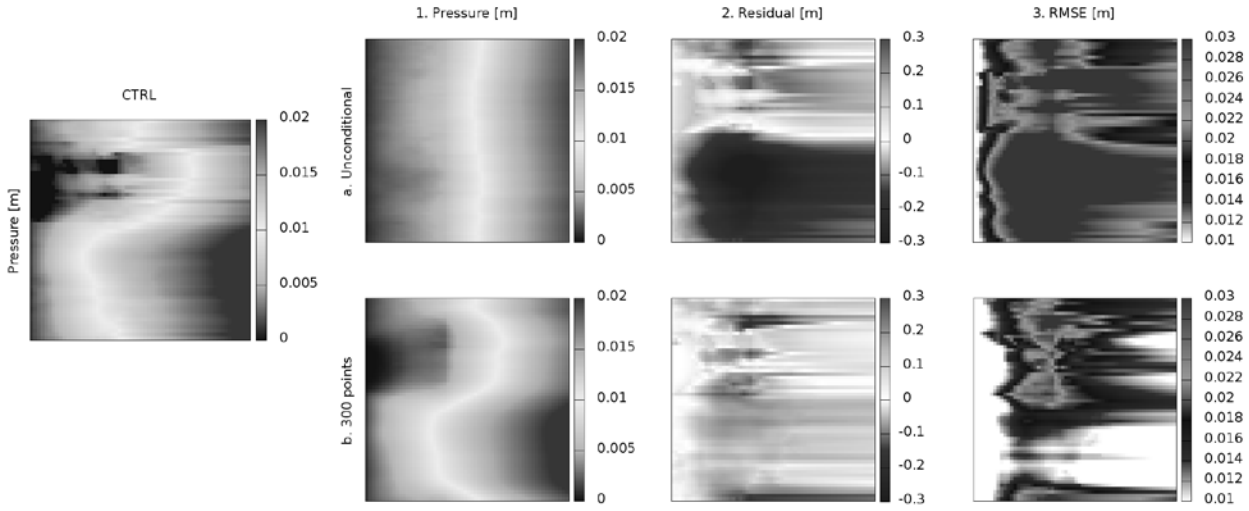

Fig. 3 Land surface pressure head for the baseflow conditioning cases at t/ta = 1.0. Plot a for the unconditional case, plot b is for 300 conditioning points. Column 1 is the ensemble average land surface pressure head, column 2 is the residual between the CTRL case and the ensemble average and column 3 is RMSE between the CTRL case and the conditioning case.

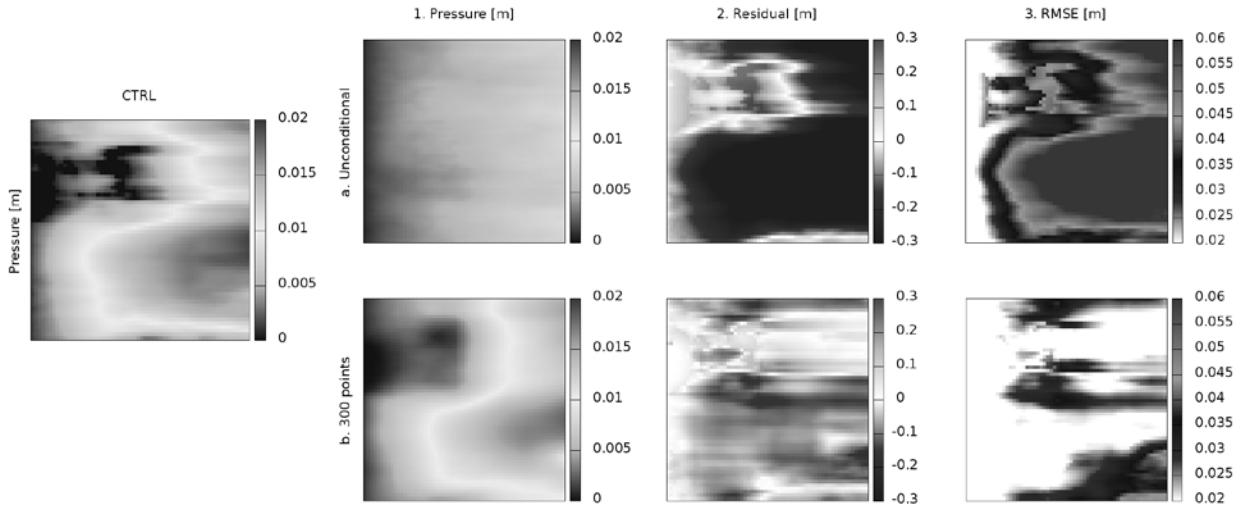

Fig. 4 Land surface pressure head for the overland flow conditioning cases at *t/ta* = 1.0. Plot a for the unconditional case, plot b is for 300 conditioning points. Column 1 is the ensemble average land surface pressure head, column 2 is the residual between the CTRL case and the ensemble average and column 3 is the RMSE between the CTRL case and the conditioning case.

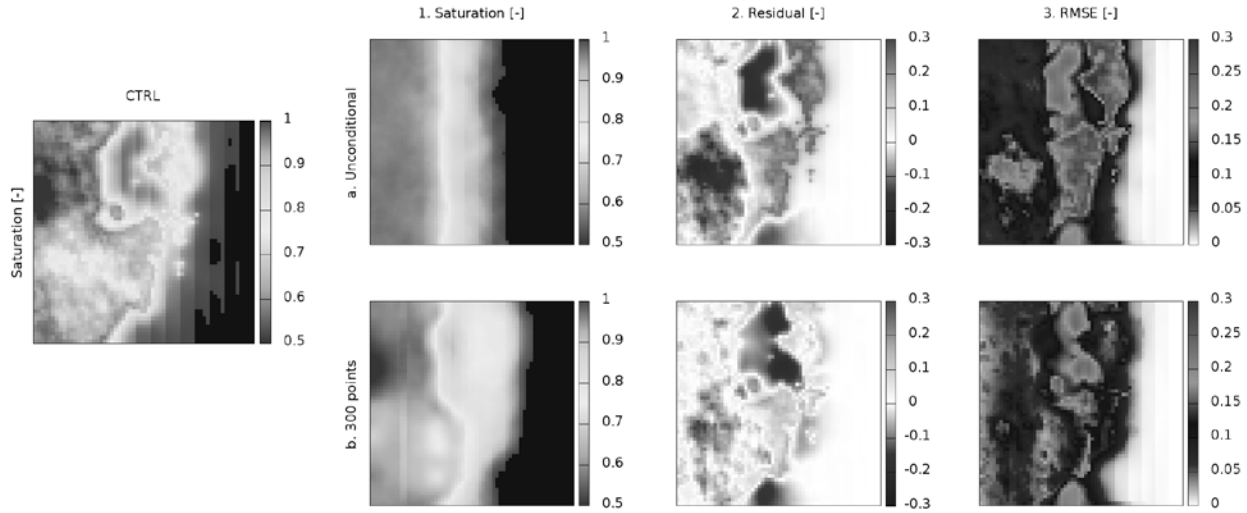

Fig. 5 Land surface saturation for the baseflow conditioning cases at *t/ta* = 4.0. Plot a for the unconditional case, plot b is for 300 conditioning points. 1 is the ensemble average land surface saturation, 2 is the residual between the CTRL case and the ensemble average and 3 is the RMSE between the CTRL case and the conditioning case.

Fig. 6), after the rainstorm, the spatial structure of the difference between the CTRL and conditioning case is representative of the hydraulic conductivity (Fig. 2).

For each conditional case outflow was recorded and averaged over the ensembles then compared to the CTRL. Figure 7 plots the resulting hydrographs for each of the cases (unconditional and 300 points) for overland (Fig. 7 Row 1) and baseflow (Fig. 7 Row 2). In the unconditional cases for overland flow it can be seen that the variance from the maximum flow to lowest flow realization is quite large and that the average of the conditional cases is drastically different from the CTRL case. With increasing data assimilation, at 300 points we see the ensemble average outflow more closely matches the CTRL case. In this figure we also see that the variance of outflows produced by each ensemble encompasses the CTRL much more closely. Variance in outflow for the baseflow case is less than the overland case outflow; this is a result of baseflow hydrographs reflecting effective behaviour and capturing the outflow for each individual realization (Meyerhoff & Maxwell, 2011).

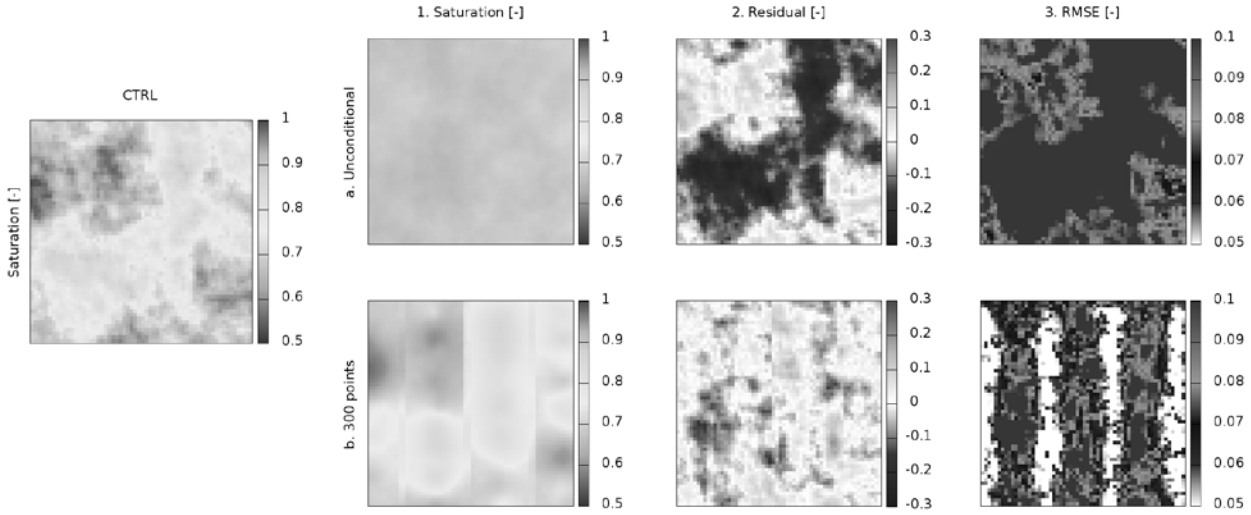

Fig. 6 Land surface saturation for the overland flow conditioning cases at *t/ta* = 2.0. Plot a for the unconditional case, plot b is for 300 conditioning points. Column 1 is the ensemble average land surface saturation, Column 2 is the residual between the CTRL case and the ensemble average and Column 3 is the RMSE between the CTRL case and the conditioning case.

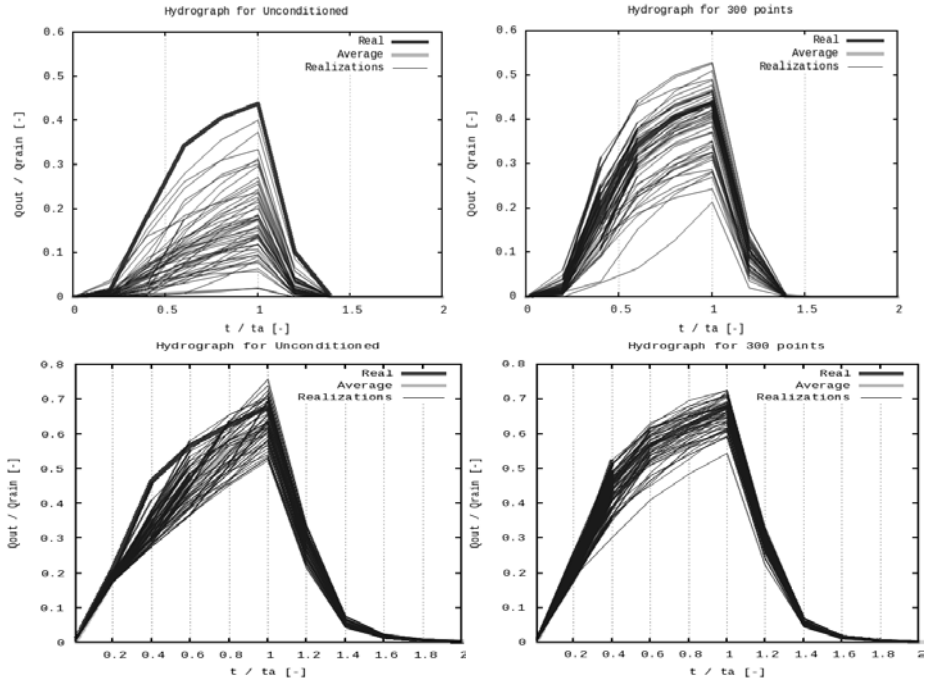

Fig. 7 Overland flow (Row 1) and Baseflow (Row 2) hydrographs for each of the conditionals case (unconditional, 75 , 150 and 300 points). Thick black lines represent the CTRL case flow, thick grey is the averaged ensemble outflow, and black lines are each individual realization.

CONCLUSION

In this study we used the fully coupled hydrologic model ParFlow to simulate groundwater and surface water flow to determine how subsurface characterization of permeability affects runoff prediction. Two separate control cases, overland (Hortonian flow) and baseflow (mixture of Dunne and Hortonian flow) were simulated. Hydraulic conductivity from the control cases was assimilated into an ensemble of realizations with increasing data density (unconditional, 75, 150 and 300 points). The ensembles of realizations were compared to the CTRL cases to determine

how increasing data assimilation affects runoff, saturation and pressure head. The hillslope used was idealized, using constant rain and hillslope, however, from this study the following conclusions were reached:

(1) Hydrograph uncertainty was reduced with increasing data assimilation for both overland and baseflow cases (Fig. 7), where the averaged ensemble flow more closely resembles the CTRL case flow. In overland cases a larger reduction in variance is seen between the realization cases.
(2) Spatial uncertainty in both land surface saturation and pressure show a decrease in difference with increasing data assimilation. Large-scale patterns of both pressure head and saturation were greater resolved with increasing data assimilation. This shows that reducing subsurface saturated hydraulic conductivity uncertainty propagates through a coupled flow system to both saturation and pressure head (Figs 3–6).
(3) We see that conditioning of the land surface shows a propagation of reduced difference and error downslope of the conditioning points in baseflow cases (Fig. 3). Pressure head showed no spatial structure correlation to the reduction in uncertainty for saturated hydraulic conductivity.
(4) Residual errors in the land surface pressure head and saturation were reduced with increasing data assimilation (Figs 3–6). This was seen for both the overland and baseflow cases.

REFERENCES

Ashby, S. F. & Falgout, R. D. (1996) A parallel multigrid preconditioned conjugate gradient algorithm for groundwater flow simulations. *Nucl. Sci. Engng* 124(1), 145–159.

Jones, J. E. & Woodward, C. S. (2001) Newton-Krylov-multigrid solvers for large-scale, highly heterogeneous, variably saturated flow problems. *Adv. Water Resour.* 24, 763–774.

Kollet, S. J. & Maxwell, R. M. (2006) Integrated surface-groundwater flow modeling: a free surface overland flow boundary condition in a parallel groundwater flow model. *Adv Water Resour*. 29(7), 945–958.

Maxwell, R. M. & Kollet, S. J. (2008) Quantifying the effects of three-dimensional subsurface heterogeneity on Hortonian runoff processes using a coupled numerical stochastic approach. *Adv. Water Resour.* 31, 807–817.

Meyerhoff, S. B. & Maxwell, R. M. (2011) Quantifying the effects of subsurface heterogeneity on hillslope runoff using a stochastic approach. *Hydrogeology J.* doi: 10.1007/s10040-011-0753-y.

Rihani, J. F. & Maxwell, R. M. & Chow, F. K. (2010) Coupling groundwater and land surface processes: Idealized simulations to identify effects of terrain and subsurface heterogeneity on land surface energy fluxes. *Water Resour. Res*. 46.

Rubin, Y. (2003) *Applied Stochastic Hydrogeology*. Oxford University Press.

Rubin, Y. & Dagan, G. (1992) Conditional estimation of solute travel time in heterogeneous formations: Impact of transmissivity measurements. *Water Resour. Res.* 28(4), 1033–1040.

Tompson, A. F. B. & Ababou, R. & Gelhar, L. W. (1989) Implementation of the three-dimensional turning bands random field generator. *Water Resour Res*. 25(10), 2227–2243.

Van Genuchten, M. T. (1980) A closed-form equation for predicting the hydraulic conductivity of unsaturated soils. *Soil Sci. Soc. Am. J*. 44, 892–898.